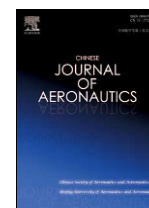




Contents lists available at ScienceDirect

Chinese Journal of Aeronauticsjournal homepage: www.elsevier.com/locate/cja

Linear Quadratic Differential Game Strategies with Two-pursuit Versus Single-evader

LIU Yanfang, QI Naiming*, TANG Zhiwei

School of Astronautics, Harbin Institute of Technology, Harbin 150001, China

Received 14 July 2011; revised 29 August 2011; accepted 12 December 2011

Abstract

In order to intercept the future targets that are characterized by high maneuverability, multiple interceptors may be launched and aimed at single target. The scenario of two missiles P and Q intercepting a single target is modeled as a two-pursuit single-evader non-zero-sum linear quadratic differential game. The intercept space is decomposed into three subspaces which are mutually disjoint and their union covers the entire intercept space. The effect of adding the second interceptor arises in the intercept space of both P and Q (PQ -intercept space). A guidance law is derived from the Nash equilibrium strategy set (NESS) of the game. Simulation studies are focused on the PQ -intercept space. It is indicated that 1) increasing the target's maneuverability will enlarge PQ -intercept space; 2) the handover conditions will be released if the initial zero-effort-miss (ZEM) of both interceptors has opposite sign; 3) overvaluation of the target's maneuverability by choosing a small weight coefficient will generate robust performance with respect to the target maneuvering command switch time and decrease the fuel requirement; and 4) co-operation between interceptors increases the interception probability.

Keywords: missile; linear quadratic differential games; two-pursuit single-evader; interception; guidance

1. Introduction

The future targets such as tactical ballistic missile (TBM), supersonic cruise missile (SCM) and unmanned aerial vehicle (UAV) are characterized by low observability and high maneuverability. The interceptor does not have substantial advantage in speed, maneuverability and agility against these targets. However, successfully intercepting such a target demands a very small miss distance or even a direct hit.

In order to successfully intercept such targets, two types of efforts can be made: 1) increasing the single-shot kill probability (SSKP) by improving navigation, guidance and control systems; 2) utilizing multiple missiles to intercept single target. This paper focuses on the end-game guidance problem of intercept-

ing single target with two interceptors.

Differential game theory is based on classical game theory and optimal control theory and is utilized to study the optimal strategies in games of two or multiple players, which is also applied to guidance law development. In the differential game model, the interceptor tries to minimize the miss distance and the target tries to maximize it. The Nash equilibrium strategy set (NESS) is the optimal guidance strategies for both players. Gutman and Leitmann^[1] studied such formulation of a scenario with the assumption that two players have constant velocities, constant maximum accelerations and ideal dynamics. The scenario was later extended to include first-order pursuer dynamics^[2-3] and evader dynamics^[4], and yielded the bounded differential game guidance laws DGL/0 and DGL/1, respectively. A vector form of differential game guidance law with the first-order pursuer and evader dynamics taken into account was studied by Chen^[5] and that with uncertainty was discussed by Wang^[6]. The effects of lateral acceleration limits on the homing performance were investigated by Hou^[7]. Shinar, et al. pro-

*Corresponding author. Tel.: +86-451-86418119.

E-mail address: qinmok@163.com

Foundation item: Ministry Level Project

posed guidance law DGL/C^[8-9] with the delay of the target's acceleration estimation and DGL/E^[10] with time-varying velocities and acceleration limits and later, with both the delay and time-varying properties combined, they developed DGL/EC^[11]. Li, et al.^[12-13] proposed a differential game guidance law for a low-altitude endoatmospheric interceptor with a forward reaction control system (RCS) and aerodynamic tail control surfaces. Under the conditions of large initial flight path error and long intercept time, with the angular nonlinearity taken into consideration, a guidance law with nonlinear differential game formulation was proposed by Liu, et al.^[14].

However, the guidance laws presented in the above papers are based on the single-pursuer single-evader differential game formulation. In the end-game guidance problem with multiple interceptors and single target, the formulation becomes multiple-pursuer single-evader game. The problem of protecting a target aircraft from a homing missile by launching a defending missile was formulated as zero-sum multiple-players game model by Perelman, et al.^[15], from which a cooperative linear quadratic differential game guidance law was yielded. The attacking missile is chasing the evading target that at some point launches a defending missile to intercept the incoming threat. Shima^[16] proposed optimal cooperation pursuit-evasion strategies for the same aircraft protecting problem, assuming that the incoming missile is using a known linear guidance law and with linear kinematics, linear dynamics and perfect information. However, this aircraft protecting problem is different from the multiple-pursuit single-evader problem. A general model and solution of multiple-pursuit single-evader game were given by Foley^[17] and Lin^[18], et al. gave the distributed non-zero-sum Nash strategies. This paper focuses on the end-game guidance problem of intercepting single target with two missiles. The engagement is modeled as non-zero-sum two-pursuit single-evader game formulation and a guidance law is derived from NESS of the game. Effective navigation gains and information sharing are also studied. The homing performance of the proposed guidance law is tested based on Monte Carlo simulation.

2. Problem Formulation

The problem dealt in this paper consists of three entities, interceptors P and Q and target T . The missiles chase the evading target while the target maneuvers to escape. The engagement between the missile P (Q) and target T is denoted as PT (QT). A roll controlled interceptor is considered in this paper. For the relatively short time interval of the end-game (with small changes in the flight direction), the motion of such an interceptor can be separated into two perpendicular channels and the guidance problem can be treated as planar in each of these channels^[12, 14, 19-20]. A sche-

matic view of the planar end-game geometry is shown in Fig. 1, where $X_1O_1Y_1$ is a Cartesian inertial reference frame. The speed, normal acceleration and flight-path angle are denoted by V , a and γ , respectively. The range between the adversaries is r and λ is the angle between line-of-sight (LOS) and X_1 axis. The subscript "0" denotes initial. The mathematical model is outlined below based on the following assumptions^[1-4, 12-14]:

- 1) Planar engagement;
- 2) Constant speed;
- 3) Perfect information structure;
- 4) Small angle deviation linearization;
- 5) Without account for gravity;
- 6) Ideal dynamics of adversaries, i.e. zero-lag.

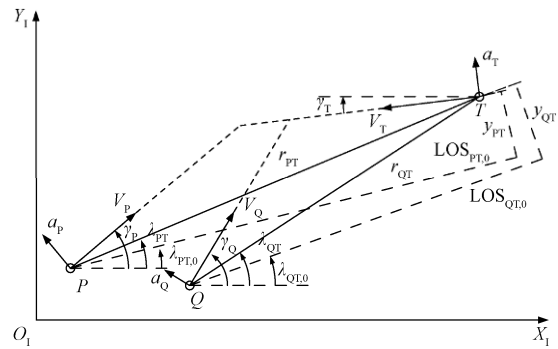


Fig. 1 End-game geometry between missiles and target.

Remark 1^[10, 21] The Assumption 3) includes two parts: the designers of both missiles have perfect knowledge of the engagement parameters and both missiles can accurately measure all of the state variables. Although in reality, the target, i.e. TBM, has no information about the interceptor's state variables, it may carry out a very close realization of the optimal interception avoidance strategy if it maneuvers randomly. Thus, the second part of Assumption 3) represents the worst case for the interceptor.

Based on Assumptions 2) and 4), the final time of the engagement PT and QT can be computed for any given initial conditions of the end-game:

$$t_{t,PT} = r_{PT,0} / (V_T \cos \varphi_{PT,0} + V_P \cos \varphi_{P,0}) \quad (1)$$

$$t_{t,QT} = r_{QT,0} / (V_T \cos \varphi_{QT,0} + V_Q \cos \varphi_{Q,0}) \quad (2)$$

where the subscripts "PT" and "QT" represents the parameters of T with respect P and Q , φ denotes the leading angle, defined as

$$\varphi_P = \gamma_P - \lambda_{PT} \quad (3)$$

$$\varphi_Q = \gamma_Q - \lambda_{QT} \quad (4)$$

$$\varphi_{PT} = \gamma_T + \lambda_{PT} \quad (5)$$

$$\varphi_{QT} = \gamma_T + \lambda_{QT} \quad (6)$$

Assume that the engagement QT is ended before PT , i.e.

$$t_{f,PT} > t_{f,QT} \tag{7}$$

allowing the final time of the game to be defined by

$$t_f = t_{f,PT} \tag{8}$$

The linearized relative motion normal to the initial LOS_{PT,0} and LOS_{QT,0} is expressed as

$$\begin{cases} \ddot{y}_{PT} = a_T \cos \varphi_{PT,0} - a_P \cos \varphi_{P,0} \\ \ddot{y}_{QT} = a_T \cos \varphi_{QT,0} - a_Q \cos \varphi_{Q,0} \end{cases} \tag{9}$$

where y_{PT} (y_{QT}) denotes the relative displacement between P (Q) and T , normal to LOS_{PT,0} (LOS_{QT,0}).

In order to reflect the disappearance of missile Q after the terminal of engagement QT , the zero-effort-miss (ZEM) z_Q is forced to remain constant for $t_{f,QT} < t < t_{f,PT}$ by forcing $\ddot{y}_{QT} = 0$ ^[15]. Thus, the relative motion equations are rewritten as

$$\begin{cases} \ddot{y}_{PT} = a_T \cos \varphi_{PT,0} - a_P \cos \varphi_{P,0} \\ \ddot{y}_{QT} = (a_T \cos \varphi_{QT,0} - a_Q \cos \varphi_{Q,0})\delta(t) \end{cases} \tag{10}$$

where

$$\delta(t) = \begin{cases} 1 & t \leq t_{f,QT} \\ 0 & t > t_{f,QT} \end{cases} \tag{11}$$

Thus, the game can be treated under unified time with final time defined in Eq. (8) and the time-to-go can be defined by

$$t_{go} = t_f - t \tag{12}$$

The relative motion in Eq. (10) can be expressed by a compact form as time-invariant, vector differential equation:

$$\dot{\mathbf{x}} = \mathbf{A}\mathbf{x} + \mathbf{B}_P u_P + \mathbf{B}_Q u_Q + \mathbf{B}_T u_T \tag{13}$$

where u is the acceleration command, the state vector is

$$\mathbf{x}^T = [y_{PT} \quad \dot{y}_{PT} \quad y_{QT} \quad \dot{y}_{QT}] \tag{14}$$

and

$$\left\{ \begin{aligned} \mathbf{A} &= \begin{bmatrix} 0 & 1 & 0 & 0 \\ 0 & 0 & 0 & 0 \\ 0 & 0 & 0 & 1 \\ 0 & 0 & 0 & 0 \end{bmatrix}, & \mathbf{B}_P &= \begin{bmatrix} 0 \\ -\cos \varphi_{P,0} \\ 0 \\ 0 \end{bmatrix} \\ \mathbf{B}_Q &= \begin{bmatrix} 0 \\ 0 \\ 0 \\ -\delta(t) \cos \varphi_{Q,0} \end{bmatrix}, & \mathbf{B}_T &= \begin{bmatrix} 0 \\ \cos \varphi_{PT,0} \\ 0 \\ \delta(t) \cos \varphi_{QT,0} \end{bmatrix} \end{aligned} \right. \tag{15}$$

ZEM is the miss distance if players will not apply any further acceleration commands. Using the transition matrix associated with Eq. (13), the ZEM vector is defined as

$$\mathbf{z} = \mathbf{D}\Phi(t_f, t)\mathbf{x}(t) \tag{16}$$

where $\mathbf{z} = [z_P \quad z_Q]^T$ with z_P and z_Q representing ZEM of P and Q , and the transition matrix is

$$\Phi(t_f, t) = \begin{bmatrix} 1 & t_{go} & 0 & 0 \\ 0 & 1 & 0 & 0 \\ 0 & 0 & 1 & t_{go} \\ 0 & 0 & 0 & 1 \end{bmatrix} \tag{17}$$

and

$$\mathbf{D} = \begin{bmatrix} 1 & 0 & 0 & 0 \\ 0 & 0 & 1 & 0 \end{bmatrix} \tag{18}$$

The dynamic of ZEM vector is

$$\dot{\mathbf{z}}(t) = \bar{\mathbf{B}}_P u_P + \bar{\mathbf{B}}_Q u_Q + \bar{\mathbf{B}}_T u_T \tag{19}$$

where

$$\begin{cases} \bar{\mathbf{B}}_P = \mathbf{D}\Phi(t_f, t)\mathbf{B}_P \\ \bar{\mathbf{B}}_Q = \mathbf{D}\Phi(t_f, t)\mathbf{B}_Q \\ \bar{\mathbf{B}}_T = \mathbf{D}\Phi(t_f, t)\mathbf{B}_T \end{cases} \tag{20}$$

The missiles P and Q are assumed to be the same and intercept the target independently. The objective of each missile is to choose its control so as to minimize the miss distance while the objective of the target is to maximize the minimum value of these two miss distances. The players' control variables are limited by imposing integral quadratic constraints. Thus, the performance criteria are

$$J_P = \frac{\alpha}{2} z_P^2(t_f) + \frac{1}{2} \int_0^{t_f} u_P^2 dt \tag{21}$$

$$J_Q = \frac{\alpha}{2} z_Q^2(t_f) + \frac{1}{2} \int_0^{t_f} u_Q^2 dt \tag{22}$$

$$J_T = -\frac{\alpha_T}{2} \min\{z_P^2(t_f), z_Q^2(t_f)\} + \frac{\beta_T}{2} \int_0^{t_f} u_T^2 dt \tag{23}$$

where the weights α , α_T , and β_T are all positive. This differential game defined by Eqs. (19)-(23) is referred to as \mathcal{G} .

3. Nash Equilibrium Strategies

The admissible controls for P , Q and T are taken as the set of piecewise continuous functions. An NESS for \mathcal{G} is defined as follows.

Definition 1^[18] The admissible strategy set (u_P^*, u_Q^*, u_T^*) is a NESS for \mathcal{G} if

$$J_P(u_P^*, u_Q^*, u_T^*) \leq J_P(u_P, u_Q^*, u_T^*) \tag{24}$$

$$J_Q(u_P^*, u_Q^*, u_T^*) \leq J_Q(u_P^*, u_Q, u_T^*) \tag{25}$$

$$J_T(u_P^*, u_Q^*, u_T^*) \leq J_T(u_P^*, u_Q^*, u_T) \tag{26}$$

for all admissible u_P, u_Q and u_T .

In order to apply the existence theory, J_T is required

to be a continuous function, which is obviously not the case for the game \mathcal{G} . This difficulty is overcome by redefining the target's performance criteria as

$$\bar{J}_T = -\frac{\alpha_T}{2}[\kappa z_p^2(t_f) + (1-\kappa)z_Q^2(t_f)] + \frac{\beta_T}{2} \int_0^{t_f} u_T^2 dt, \quad 0 \leq \kappa \leq 1 \quad (27)$$

Obviously, the criteria Eq. (27) is equivalent to Eq. (23) if the variable κ satisfies

$$\kappa = \begin{cases} 0 & z_p^2(t_f) > z_Q^2(t_f) \\ \sigma & z_p^2(t_f) = z_Q^2(t_f), 0 \leq \sigma \leq 1 \\ 1 & z_p^2(t_f) < z_Q^2(t_f) \end{cases} \quad (28)$$

The differential game defined by Eqs. (19)-(22) and Eq. (27) is referred to as $\bar{\mathcal{G}}$.

The Hamiltonian of the game $\bar{\mathcal{G}}$ is

$$\begin{cases} H_P = \lambda_P^T \dot{z}(t) + \frac{1}{2} u_P^2 \\ H_Q = \lambda_Q^T \dot{z}(t) + \frac{1}{2} u_Q^2 \\ H_T = \lambda_T^T \dot{z}(t) + \frac{1}{2} \beta_T u_T^2 \end{cases} \quad (29)$$

with the adjoint variables satisfying

$$F = [I + \int_t^{t_f} (\bar{B}_P \bar{B}_P^T A_P + \bar{B}_Q \bar{B}_Q^T A_Q + \bar{B}_T \bar{B}_T^T A_T / \beta_T) d\tau]^{-1} = \frac{3}{\Theta t_{go}^3} \begin{bmatrix} 3/t_{go}^3 + \alpha \cos^2 \varphi_{Q,0} - [\alpha_T(1-\kappa)\delta^2(t) \cos^2 \varphi_{QT,0}] / \beta_T & [\alpha_T(1-\kappa) \cos \varphi_{PT,0} \cos \varphi_{QT,0}] / \beta_T \\ (\alpha_T \kappa \delta(t) \cos \varphi_{PT,0} \cos \varphi_{QT,0}) / \beta_T & 3/t_{go}^3 + \alpha \cos^2 \varphi_{P,0} - (\alpha_T \kappa \cos^2 \varphi_{PT,0}) / \beta_T \end{bmatrix} \quad (34)$$

$$\Theta = [3/t_{go}^3 + \alpha \cos^2 \varphi_{P,0} - (\alpha_T \kappa \cos^2 \varphi_{PT,0}) / \beta_T] \{3/t_{go}^3 + \alpha \cos^2 \varphi_{Q,0} - [\alpha_T(1-\kappa)\delta^2(t) \cos^2 \varphi_{QT,0}] / \beta_T\} - [\alpha_T^2 \kappa(1-\kappa) \delta(t) \cos^2 \varphi_{PT,0} \cos^2 \varphi_{QT,0}] / \beta_T^2 \quad (35)$$

A sufficient condition for the existence of NESS is

$$\Theta \neq 0 \quad (36)$$

The closed form solution is obtained by substituting Eq. (33) into Eq. (30) and then into Eq. (31):

$$\begin{cases} u_P^* = -\alpha \bar{B}_P^T A_P Fz(t) \\ u_Q^* = -\alpha \bar{B}_Q^T A_Q Fz(t) \\ u_T^* = \alpha_T \bar{B}_T^T A_T Fz(t) / \beta_T \end{cases} \quad (37)$$

Definition 2 The intercept space \mathcal{S} is a set of $z(t)$, i.e.

$$\mathcal{S} = \{z(t)\} \quad (38)$$

Definition 3 The P -intercept space \mathcal{S}_P is a subset of \mathcal{S} satisfying

$$\mathcal{S}_P = \{z(t) \mid (Fz(t))^T (A_P - A_Q)(Fz(t)) < 0, \quad \forall 0 \leq \kappa \leq 1\} \quad (39)$$

Definition 4 The Q -intercept space \mathcal{S}_Q is a sub-

$$\begin{cases} \lambda_P(t) = \alpha A_P z(t_f) \\ \lambda_Q(t) = \alpha A_Q z(t_f) \\ \lambda_T(t) = -\alpha_T A_T z(t_f) \end{cases} \quad (30)$$

and open-loop optimal controllers to be

$$\begin{cases} u_P^* = -\lambda_P^T \bar{B}_P \\ u_Q^* = -\lambda_Q^T \bar{B}_Q \\ u_T^* = -\lambda_T^T \bar{B}_T / \beta_T \end{cases} \quad (31)$$

where

$$\begin{cases} A_P = \begin{bmatrix} 1 & 0 \\ 0 & 0 \end{bmatrix} \\ A_Q = \begin{bmatrix} 0 & 0 \\ 0 & 1 \end{bmatrix} \\ A_T = \begin{bmatrix} \kappa & 0 \\ 0 & 1-\kappa \end{bmatrix} \end{cases} \quad (32)$$

Substituting the open-loop optimal controllers (31) into Eq. (19) and integrating from t to t_f , the linear but coupled algebraic equations of $z(t_f)$ is obtained:

$$z(t_f) = Fz(t) \quad (33)$$

where

set of \mathcal{S} satisfying

$$\mathcal{S}_Q = \{z(t) \mid (Fz(t))^T (A_P - A_Q)(Fz(t)) > 0, \quad \forall 0 \leq \kappa \leq 1\} \quad (40)$$

Definition 5 The PQ -intercept space \mathcal{S}_{PQ} is a subset of \mathcal{S} satisfying

$$\mathcal{S}_{PQ} = \{z(t) \mid \exists 0 \leq \kappa \leq 1, \quad (Fz(t))^T (A_P - A_Q)(Fz(t)) = 0\} \quad (41)$$

Obviously, \mathcal{S}_P , \mathcal{S}_Q and \mathcal{S}_{PQ} are disjoint and their union covers the entire intercept space \mathcal{S} , i.e.

$$\mathcal{S}_P \cap \mathcal{S}_Q = \mathcal{S}_P \cap \mathcal{S}_{PQ} = \mathcal{S}_Q \cap \mathcal{S}_{PQ} = \emptyset \quad (42)$$

and

$$\mathcal{S}_P \cup \mathcal{S}_Q \cup \mathcal{S}_{PQ} = \mathcal{S} \quad (43)$$

Theorem 1 If the inequality in Eq. (36) is satisfied for all $0 \leq \kappa \leq 1$, and

- 1) $z(t) \in \mathcal{S}_P$, then Eq. (37) is a NESS for game \mathcal{G}

when $\kappa = 1$.

2) $z(t) \in \mathcal{S}_Q$, then Eq. (37) is a NESS for game \mathcal{G} when $\kappa = 0$.

3) $z(t) \in \mathcal{S}_{PQ}$, then Eq. (37) is a NESS for game \mathcal{G} when κ satisfies $(Fz(t))^T(A_P - A_Q)(Fz(t)) = 0$.

Proof The strategy in Eq. (37) is a NESS for the game $\bar{\mathcal{G}}$ if inequalities in Eq. (36) are satisfied. Thus,

$$J_P(u_P^*, u_Q^*, u_T^*) \leq J_P(u_P, u_Q^*, u_T^*) \quad (44)$$

$$J_Q(u_P^*, u_Q^*, u_T^*) \leq J_Q(u_P^*, u_Q, u_T^*) \quad (45)$$

$$\bar{J}_T(u_P^*, u_Q^*, u_T^*) \leq \bar{J}_T(u_P^*, u_Q^*, u_T) \quad (46)$$

To show that Eq. (37) is a NESS for \mathcal{G} , one only needs to verify the inequality in Eq. (26).

1) In the P -intercept space \mathcal{S}_P , the strategy Eq. (37) guarantees $(Fz(t))^T(A_P - A_Q)(Fz(t)) < 0$, namely, $z_P^2(t_f) < z_Q^2(t_f)$. As $0 \leq \kappa \leq 1$, then

$$(1 - \kappa)z_P^2(t_f) \leq (1 - \kappa)z_Q^2(t_f) \quad (47)$$

Adding $\kappa z_P^2(t_f) - \beta_T \int_0^{t_f} u_T^2 dt$ to both sides of Eq. (47) and multiplied by $-1/2$, one obtains

$$\begin{aligned} & -\frac{\alpha_T}{2}[\kappa z_P^2(t_f) + (1 - \kappa)z_Q^2(t_f)] + \frac{\beta_T}{2} \int_0^{t_f} u_T^2 dt \leq \\ & -\frac{\alpha_T}{2}z_P^2(t_f) + \frac{\beta_T}{2} \int_0^{t_f} u_T^2 dt \end{aligned} \quad (48)$$

As $z_P^2(t_f) < z_Q^2(t_f)$, Eq. (48) is equivalent to

$$\bar{J}_T(u_P^*, u_Q^*, u_T) \leq J_T(u_P^*, u_Q^*, u_T) \quad (49)$$

when $\kappa = 1$,

$$J_T(u_P^*, u_Q^*, u_T^*) = \bar{J}_T(u_P^*, u_Q^*, u_T^*) \quad (50)$$

From Eq. (46) and Eqs. (49)-(50), we get

$$J_T(u_P^*, u_Q^*, u_T^*) \leq J_T(u_P^*, u_Q^*, u_T) \quad (51)$$

2) In the intercept space \mathcal{S}_Q , the strategy Eq.(37) guarantees $(Fz(t))^T(A_P - A_Q)(Fz(t)) > 0$, namely, $z_P^2(t_f) > z_Q^2(t_f)$. As $0 \leq \kappa \leq 1$, then

$$(1 - \kappa)z_P^2(t_f) \geq (1 - \kappa)z_Q^2(t_f) \quad (52)$$

Adding $\kappa z_Q^2(t_f) - \beta_T \int_0^{t_f} u_T^2 dt$ to both sides of Eq. (52) and multiplied by $-1/2$, one obtains

$$\begin{aligned} & -\frac{\alpha_T}{2}[\kappa z_P^2(t_f) + (1 - \kappa)z_Q^2(t_f)] + \frac{\beta_T}{2} \int_0^{t_f} u_T^2 dt \leq \\ & -\frac{\alpha_T}{2}z_Q^2(t_f) + \frac{\beta_T}{2} \int_0^{t_f} u_T^2 dt \end{aligned} \quad (53)$$

As $z_P^2(t_f) > z_Q^2(t_f)$, Eq. (53) is equivalent to

$$\bar{J}_T(u_P^*, u_Q^*, u_T) \leq J_T(u_P^*, u_Q^*, u_T) \quad (54)$$

when $\kappa = 0$,

$$J_T(u_P^*, u_Q^*, u_T^*) = \bar{J}_T(u_P^*, u_Q^*, u_T^*) \quad (55)$$

From Eq. (46) and Eqs. (54)-(55), we get

$$J_T(u_P^*, u_Q^*, u_T^*) \leq J_T(u_P^*, u_Q^*, u_T) \quad (56)$$

3) In the intercept space \mathcal{S}_{PQ} , there exists $0 \leq \kappa \leq 1$ such that the optimal strategy in Eq. (37) satisfies $(Fz(t))^T(A_P - A_Q)(Fz(t)) = 0$, i.e. $z_P^2(t_f) = z_Q^2(t_f)$. Then, for that κ ,

$$J_T(u_P^*, u_Q^*, u_T^*) = \bar{J}_T(u_P^*, u_Q^*, u_T^*) \quad (57)$$

Let the missiles P and Q play the strategy in Eq. (37) and the target play any admissible strategy u_T . One of three possibilities may arise and each is considered individually.

If $z_P^2(t_f) > z_Q^2(t_f)$, then

$$(1 - \kappa)z_P^2(t_f) \geq (1 - \kappa)z_Q^2(t_f) \quad (58)$$

Adding $\kappa z_Q^2(t_f) - \beta_T \int_0^{t_f} u_T^2 dt$ to both sides of Eq. (58) and multiplied by $-1/2$, one obtains

$$\begin{aligned} & -\frac{\alpha_T}{2}[\kappa z_P^2(t_f) + (1 - \kappa)z_Q^2(t_f)] + \frac{\beta_T}{2} \int_0^{t_f} u_T^2 dt \leq \\ & -\frac{\alpha_T}{2}z_Q^2(t_f) + \frac{\beta_T}{2} \int_0^{t_f} u_T^2 dt \end{aligned} \quad (59)$$

As $z_P^2(t_f) > z_Q^2(t_f)$, Eq. (59) is equivalent to

$$\bar{J}_T(u_P^*, u_Q^*, u_T) \leq J_T(u_P^*, u_Q^*, u_T) \quad (60)$$

From Eq. (46), Eq. (57) and Eq. (60), we get

$$J_T(u_P^*, u_Q^*, u_T^*) \leq J_T(u_P^*, u_Q^*, u_T) \quad (61)$$

Cases $z_P^2(t_f) < z_Q^2(t_f)$ and $z_P^2(t_f) = z_Q^2(t_f)$ also lead to the result

$$J_T(u_P^*, u_Q^*, u_T^*) \leq J_T(u_P^*, u_Q^*, u_T) \quad (62)$$

Theorem 1 is proved.

Remark 2 As shown before, the intercept spaces \mathcal{S}_P , \mathcal{S}_Q and \mathcal{S}_{PQ} are mutually disjoint and their union covers the entire initial state space. In space \mathcal{S}_P , the target T plays against missile P only and ignores Q ; the missile P generates a smaller miss distance. In space \mathcal{S}_Q , the target T plays against missile Q only and ignores P ; the missile Q generates a smaller miss distance. In space \mathcal{S}_{PQ} , the target T plays against both missiles; the effect of adding the second interceptor arises here. A general result is given in Ref. [17]; however, it did not show that the three spaces are disjoint and their union covers the entire space. The results given here is focused on the interception problem

of single target with two missiles, and Definitions 2-5 show that the three sub-intercept spaces are mutually disjoint and their union covers the entire initial state space.

In the following sections, the focus will be on the guidance law yielded from NESS and its implication.

4. Guidance Strategies

The guidance law can be yielded from the NESS in Eq. (37) and rewritten in the classical form

$$\begin{cases} u_P^* = N_P z(t)/t_{go}^2 \\ u_Q^* = N_Q z(t)/t_{go}^2 \\ u_T^* = N_T z(t)/t_{go}^2 \end{cases} \quad (63)$$

where N_P , N_Q and N_T are effective navigation gain vectors

$$\begin{cases} N_P = -\alpha \bar{B}_P^T A_P \bar{F} \\ N_Q = -\alpha \bar{B}_Q^T A_Q \bar{F} \\ N_T = \alpha_T \bar{B}_T^T A_T \bar{F} / \beta_T \end{cases} \quad (64)$$

and

$$\bar{F} = Ft_{go}^2 \quad (65)$$

However, when it is implicated, κ should be calculated first. The parameter κ should be chosen as 1 or 0 for the case ZEM vector $z(t)$ belonging to the P -intercept space or Q -intercept space, respectively; if $z(t) \in \mathcal{S}_{PQ}$, κ is the solution of $(Fz(t))^T (A_P - A_Q) = 0$.

4.1. Intercept space decomposition

The intercept space defined in Definitions 3-5 is computed and shown in Fig. 2. The intercept space is decomposed into three subspaces: \mathcal{S}_P , \mathcal{S}_Q and \mathcal{S}_{PQ} . It can be seen that as been proved before, the three sub-intercept spaces are mutually disjoint and their union covers the entire intercept space. A comparison about intercept space decomposition for different β_T is shown in Figs. 2-3. The PQ -intercept space enlarges with β_T decreasing. The parameter β_T represents the maneuverability of the target. A smaller weight β_T means a higher expected maneuvering capability of the target relative to that of the interceptors. Thus, the added second interceptor affects a larger region when the target has a high maneuverability. Figure 4 shows the κ value. The combination of it and Eq. (63) will determine the guidance law. In the space \mathcal{S}_{PQ} , κ increases with $|z_Q/z_P|$.

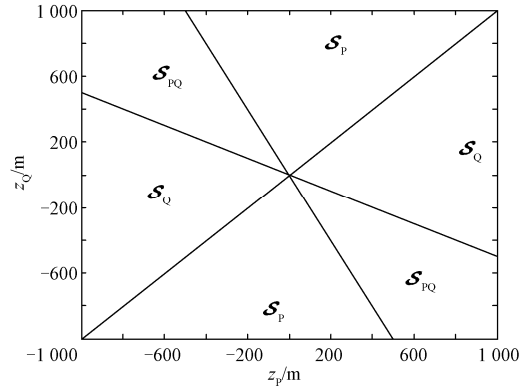


Fig. 2 Intercept space decomposition: $\beta_T = 3$.

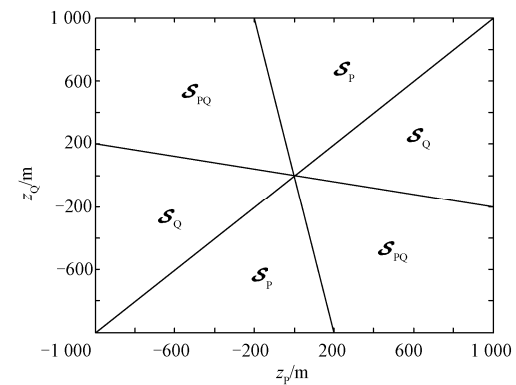


Fig. 3 Intercept space decomposition: $\beta_T = 1.5$.

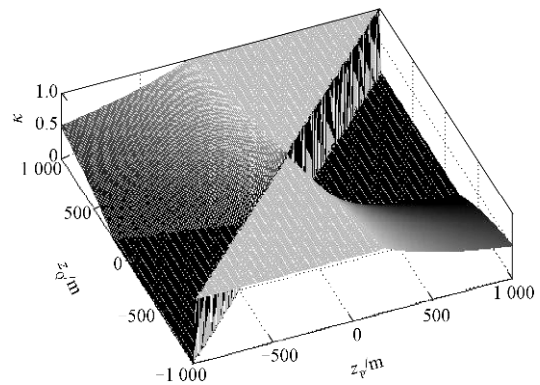


Fig. 4 κ value distribution: $\beta_T = 1.5$.

4.2. Effective navigation gain

The effective navigation gain given in Eq. (64) is a function of κ and shown in Fig. 5. Denote the i th term of the vector N as $N(i)$. The terms $N_P(1)$ and $N_Q(2)$ are responsible for intercepting the target, i.e. decreasing $z_p(t)$ and $z_Q(t)$, respectively. The term $N_P(2)$ is responsible for assisting the missile Q to intercept the target, i.e. decreasing $z_Q(t)$; the term $N_Q(1)$ is for assisting the missile P to intercept the target, i.e. decreasing $z_p(t)$. Both terms represent the coupling effects in navigation gain of the other missile. $N_T(1)$ and $N_T(2)$ are responsible for avoiding the interception of P and Q , respectively. When $\kappa = 1$, the

terms $N_P(2)$ and $N_T(2)$ are equal to zero, which verifies that the target plays against interceptor P only. However, both terms of effective navigation gain of interceptor Q , $N_Q(1)$ and $N_Q(2)$ are non-zero, that is to say, the interceptor Q tries to decrease $z_Q(t)$ and, at the same time assist P to decrease $z_P(t)$. The similar results can be obtained when $\kappa = 0$ for interceptor Q . When $0 < \kappa < 1$, i.e. $\kappa = 0.5$, the coupling terms of both P and Q are nonzero, which means both of them assist each other to reduce ZEM. The parameter κ governing the effort distribution on reducing one's own ZEM and assisting to reduce the other missile's ZEM. The results that the target has high maneuverability are also shown in Fig. 6. The effective navigation gain increases with the target's maneuverability. The term assisting the other missile to reduce ZEM becomes larger than the term reducing one's own ZEM when $\kappa = 1$ for Q and $\kappa = 0$ for P . This result shows that the effect of the adding interceptor increases with the maneuverability of the target and using two-missile or multi-missiles to intercept single-target is meaningful when the missile does not have significant maneuverability advantage over the target.

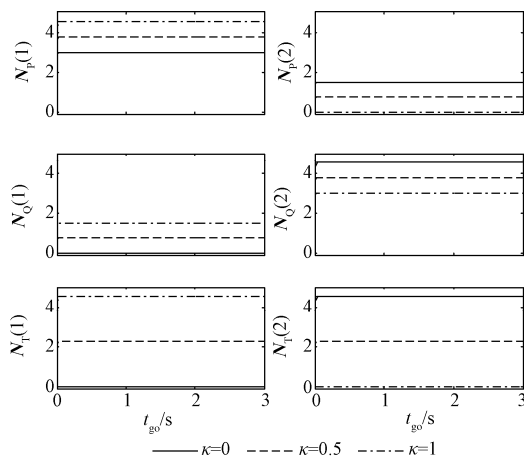


Fig. 5 Effective navigation gains: $\beta_T = 3$.

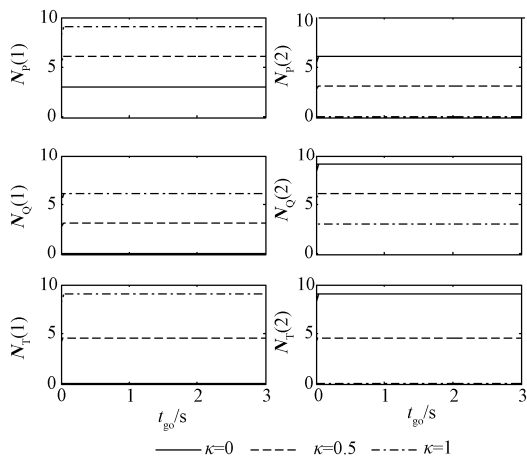


Fig. 6 Effective navigation gains: $\beta_T = 1.5$.

4.3. Game space structure

Equation (33) gives the relationship between the current ZEM vector and the terminal ZEM vector. Using this relationship, the optimal trajectories can be calculated for a given terminal ZEM vector. The family of the optimal trajectories fills the game space and is shown in Fig. 7. The norm of the terminal ZEM vector is set to be 1 m, i.e. $\|z(t_f)\| = 1$. As shown in the figure, ZEMs reduce with time, no matter from which sub-intercept space the interception starts. However, the handover condition will be released if $z_P(t_0)$ and $z_Q(t_0)$ have different signs. The reason is that, in this condition, when the target maneuvers to escape one interceptor, its effort actually reduces the ZEM of the other missile. Note that the results are yielded without considering the control saturation. The performance under control saturation is studied by simulation in Section 6.

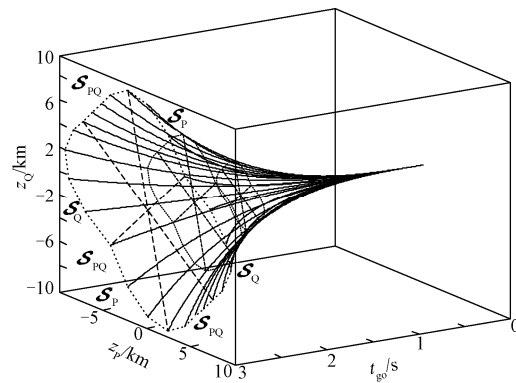


Fig. 7 Game space structure: $\beta_T = 3$.

5. Cooperation Guidance

The cooperation between different interceptors has not been taken into account in Sections 2-4. However, a higher estimation precision may be obtained by sharing information between interceptors. In this section, the sharing information and cooperative guidance are analyzed. It is assumed that the relative position between the interceptors is known by each interceptor to a very high accuracy and the measured information about that target can be shared without any delay. As stated in Remark 1, in reality, the target, i.e. TBM, has no information about the interceptors' states. In this case, both optimal control and differential game theories predict that the optimal missile avoidance maneuver has such a "bang-bang" structure as changing the maneuvering direction randomly [9-10, 21]. The target random change of maneuvering direction is approximated by white noise through an integrator [22-23]

$$\dot{u}_T = u_s \tag{66}$$

where u_s is a zero-mean white Gaussian noise proc-

ess with power spectral density $(a_T^{\max})^2 / t_f$.

The measurement equation of interceptor P is

$$\mathbf{z}_{k,P} = [r_{PT,P} \quad \lambda_{PT,P} \quad r_{QT,P} \quad \lambda_{QT,P}]^T + \mathbf{v}_{k,P} = \begin{bmatrix} r_{PT,P} \\ \lambda_{PT,P} \\ \sqrt{\Delta X_{QT}^2 + \Delta Y_{QT}^2} \\ \arctan(\Delta Y_{QT} / \Delta X_{QT}) \end{bmatrix} + \mathbf{v}_{k,P} \quad (67)$$

$$\begin{cases} \Delta X_{QT} = \Delta X_{QP} + r_{PT,P} \cos \lambda_{PT,P} \\ \Delta X_{QP} = X_P - X_Q \\ \Delta Y_{QT} = \Delta Y_{QP} + r_{PT,P} \sin \lambda_{PT,P} \\ \Delta Y_{QP} = Y_P - Y_Q \end{cases} \quad (68)$$

$$\begin{cases} \mathbf{v}_{k,P} \sim N(\mathbf{0}_{4 \times 1}, \mathbf{R}) \\ \mathbf{R} = \text{diag}\{\sigma_{rPT}^2, \sigma_{\lambda PT}^2, \sigma_{rQT}^2, \sigma_{\lambda QT}^2\} \end{cases} \quad (69)$$

The symbol X, Y represent the position of the players, \mathbf{v} represents measurement noise, and σ is standard deviation of the measurement errors.

The linearization of the measurement equation is

$$\mathbf{z}_{k,P} = \mathbf{H}_{k,P} \bar{\mathbf{x}}_k + \mathbf{v}_{k,P} \quad (70)$$

where

$$\bar{\mathbf{x}}_k = [r_{PT} \quad \lambda_{PT} \quad r_{QT} \quad \lambda_{QT}]^T \quad (71)$$

$$\mathbf{H}_{k,P} = \begin{bmatrix} 1 & 0 & 0 & 0 \\ 0 & 1 & 0 & 0 \\ \frac{\Delta_1}{r_{QT,P}} & -\frac{r_{PT,P} \Delta_2}{r_{QT,P}} & 0 & 0 \\ \frac{\Delta_2}{r_{QT,P}^2} & \frac{r_{PT,P} \Delta_1}{r_{QT,P}^2} & 0 & 0 \end{bmatrix} \quad (72)$$

$$\begin{cases} \Delta_1 = \Delta X_{QT} \cos \lambda_{PT,P} + \Delta Y_{QT} \sin \lambda_{PT,P} \\ \Delta_2 = \Delta X_{QT} \sin \lambda_{PT,P} - \Delta Y_{QT} \cos \lambda_{PT,P} \end{cases} \quad (73)$$

The linearized measurement equation of interceptor Q can also be obtained as

$$\mathbf{z}_{k,Q} = \mathbf{H}_{k,Q} \bar{\mathbf{x}}_k + \mathbf{v}_{k,Q} \quad (74)$$

where

$$\mathbf{H}_{k,Q} = \begin{bmatrix} 0 & 0 & \frac{\Delta_3}{r_{PT,Q}} & -\frac{r_{QT,Q} \Delta_4}{r_{PT,Q}} \\ 0 & 0 & \frac{\Delta_4}{r_{PT,Q}^2} & \frac{r_{QT,Q} \Delta_3}{r_{PT,Q}^2} \\ 0 & 0 & 1 & 0 \\ 0 & 0 & 0 & 1 \end{bmatrix} \quad (75)$$

$$\begin{cases} \Delta_3 = \Delta X_{PT} \cos \lambda_{QT,Q} + \Delta Y_{PT} \sin \lambda_{QT,Q} \\ \Delta_4 = \Delta X_{PT} \sin \lambda_{QT,Q} - \Delta Y_{PT} \cos \lambda_{QT,Q} \end{cases} \quad (76)$$

$$\begin{cases} \Delta X_{PT} = \Delta X_{PQ} + r_{QT,Q} \cos \lambda_{QT,Q} \\ \Delta X_{PQ} = X_Q - X_P \\ \Delta Y_{PT} = \Delta Y_{PQ} + r_{QT,Q} \sin \lambda_{QT,Q} \\ \Delta X_{PQ} = Y_Q - Y_P \end{cases} \quad (77)$$

$$\mathbf{v}_{k,Q} \sim N(\mathbf{0}_{4 \times 1}, \mathbf{R}) \quad (78)$$

Combination of Eq. (70) and Eq. (74) can generate the total measurement equation

$$\mathbf{z}_k = \mathbf{H}_k \bar{\mathbf{x}}_k + \mathbf{v}_k \quad (79)$$

where

$$\mathbf{z}_k = [\mathbf{z}_{k,P}^T \quad \mathbf{z}_{k,Q}^T]^T \quad (80)$$

$$\mathbf{H}_k = [\mathbf{H}_{k,P}^T \quad \mathbf{H}_{k,Q}^T]^T \quad (81)$$

$$\mathbf{v}_k = [\mathbf{v}_{k,P}^T \quad \mathbf{v}_{k,Q}^T]^T \quad (82)$$

By the combination of Eq. (13), Eq. (66) and Eq. (80) and using Kalman filter, the state of the engagement can be obtained.

6. Simulation

In the simulation, the initial ZEM vector $\mathbf{z}(t_0)$ is selected in the PQ -intercept space. Both interceptors utilize the guidance presented in this paper (denoted as CLQDG). The target utilizes “bang-bang” maneuvering strategy, i.e. it maneuvers with the maximum acceleration and changes its direction at a random time $(t_{go})_{sw}$. The accelerations of the target and interceptors are assumed to be bounded. Simulation parameters are given in Table 1.

Table 1 Simulation parameters

Initial parameter	Guidance parameter	State parameter
$\gamma_{P,0} = 93^\circ$,		$V_P = V_Q = 2.5 \text{ km/s}$,
$\gamma_{Q,0} = 86^\circ$,	$\alpha = 10^8$,	$V_T = 3.0 \text{ km/s}$,
$\gamma_{T,0} = -90^\circ$,	$\alpha_Q = 10^8$,	$a_T^{\max} = 200 \text{ m/s}^2$,
$\lambda_{PT,0} = 92^\circ$	$\beta_T = 1.5$,	$a_P^{\max} = a_Q^{\max} = 300 \text{ m/s}^2$
$\lambda_{QT,0} = 88^\circ$		

6.1. Performance of guidance law

The profiles of ZEM and acceleration are shown in Figs. 8-9 for $(t_{go})_{sw} = 1.2 \text{ s}$. The results when the targets utilize linear quadratic differential game (LQDG) guidance law are also shown in the figures. Seen from Fig. 9, the accelerations of interceptors P and Q are not only a function of one's own ZEM but also influenced by ZEM of the other missile. As a result, the ZEM vector moves to the origin $(z_P, z_Q) = (0, 0) \text{ m}$ with the manner that z_P almost equals z_Q .

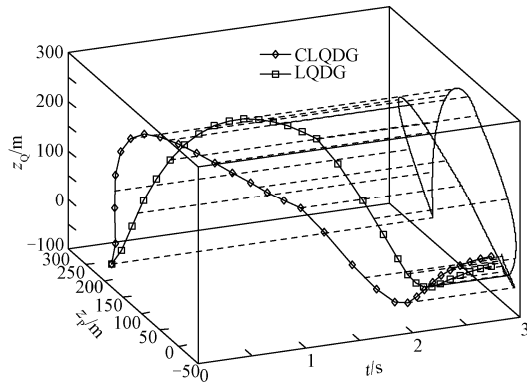


Fig. 8 ZEM vector profiles: $\beta_T = 1.5$.

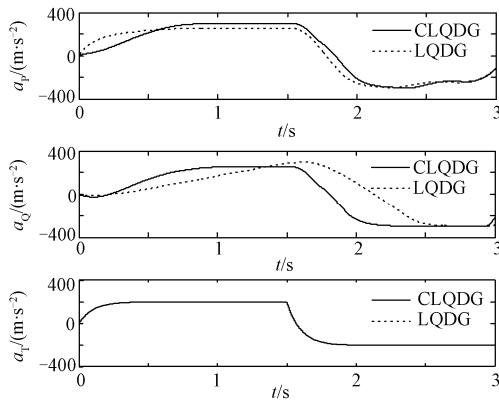


Fig. 9 Acceleration profiles: $\beta_T = 1.5$.

6.2. Robustness to target maneuver

As the target cannot obtain information about interceptors, it changes maneuver direction randomly. In different runs, $(t_{go})_{sw}$ changes in a step of 0.06 s. The miss distance is shown as a function of target's maneuvering direction switch time in Fig. 10. The miss distance is defined as the minimum miss distance of P and Q . Results with target's maneuverability estimation errors are also shown in the figure, with $\beta_T=1.2$, $\beta_T=1.5$ and $\beta_T=1.8$ representing a correct estimation, overestimation and underestimation of the target's maneuverability, respectively. The divert velocity, which represents the energy needed for the interception, is shown in Fig. 11. In the overestimation condition, the effective navigation gains increase (seen from Figs. 5-6), as a result a large acceleration command will be

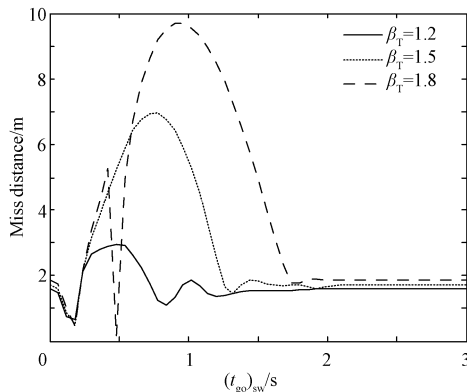


Fig. 10 Miss distance vs $(t_{go})_{sw}$.

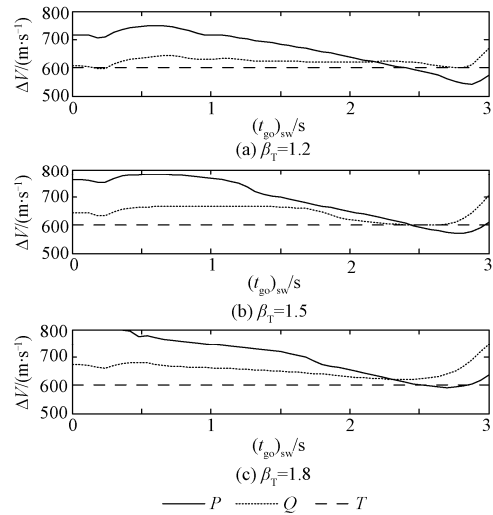


Fig. 11 Divert velocity vs $(t_{go})_{sw}$.

utilized at the beginning of the engagement and the ZEM decreases quickly. This generates a robust performance with respect to the target's maneuvering command switch time and less fuel requirement. However, seen from sufficient condition of the existence of optimal solution in Eq. (36), β_T cannot be too small.

6.3. Monte Carlo simulation

A 500-run Monte Carlo simulation study is used to test the performance of the proposed guidance law. In the simulation, the target maneuvering direction changes randomly and the simulated measurement noises are $\sigma_{rPT} = \sigma_{rQT} = 10$ m and $\sigma_{\lambda PT} = \sigma_{\lambda QT} = 1 \times 10^{-3}$ rad. The integration step is set to be 0.1 ms and the guidance cycle is selected as 10 ms. Three guidance structures, i.e., the proposed guidance law with shared information (CLQDG/S), the proposed guidance law without shared information (CLQDG) and the LQDG guidance law, were compared in the simulation. Figure 12 shows the cumulative miss distance distributions. Seen from the figure, CLQDG realizes the same miss distance with higher probability, which can release the need of the lethal radius of warhead. The sharing information increases the precision of the Kalman filter, as well as the interception probability. However, this increase is not very obvious. The sharing information

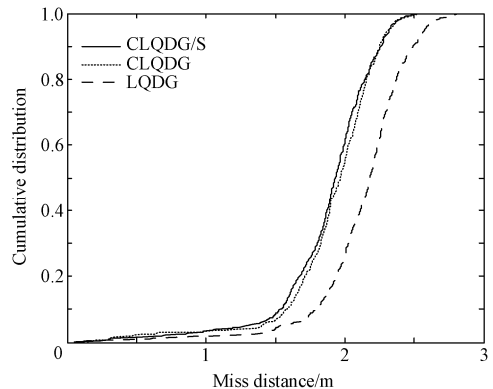


Fig. 12 Cumulative miss distance distributions.

is very useful when one of the infrared sensor or radar sensors of the interceptors is fault.

7. Conclusions

1) The interception of single target with two interceptors is modeled as a non-zero-sum two-pursuer single-evader game. The game is solved with optimal control and game theory.

2) The intercept space is decomposed into three subspaces: P -intercept space with target playing with interceptor P , Q -intercept space with target playing with interceptor Q and PQ -intercept space with target playing with both interceptors. They are mutually disjoint and their union covers the entire intercept space.

3) A guidance law yields from the NESS of the game. The effective navigation gain of each missile becomes a vector influenced by ZEM of both interceptors. The effective navigation gains increase with target's maneuverability and the PQ -intercept space enlarges, too.

4) If the initial ZEMs of both interceptors have opposite sign and both target and missiles utilize the guidance strategies proposed in this paper, the hand-over condition between the midcourse and terminal phase will be released.

5) A proper overestimation of target's maneuverability can generate robust performance with respect to the target's maneuvering command switch time and decrease the fuel requirement.

6) Monte Carlo simulation shows that the proposed guidance law realizes the same miss distance with higher probability.

References

- [1] Gutman S, Leitmann G. Optimal strategies in the neighborhood of a collision course. *AIAA Journal* 1976; 14(9): 1210-1212.
- [2] Gutman S. On optimal guidance for homing missile. *Journal of Guidance and Control* 1979; 2(4): 296-300.
- [3] Shinar J, Gutman S. Three-dimensional optimal pursuit and evasion with bounded control. *IEEE Transactions on Automatic Control* 1980; 25(3): 492-496.
- [4] Shinar J. Solution techniques for realistic pursuit-evasion game. *Advances in Control and Dynamic Systems*. New York: Academic Press, 1981: 63-124.
- [5] Chen X Y. An optimal guidance law via first order inertial loop. *Acta Aeronautica et Astronautica Sinica* 1982; 3(4): 84-92. [in Chinese]
- [6] Wang C Z. An optimal intercept guidance law with uncertain factors. *Acta Aeronautica et Astronautica Sinica* 1983; 4(4): 70-77. [in Chinese]
- [7] Hou M S. A study of differential game optimal guidance laws for air-to-air missiles. *Acta Aeronautica et Astronautica Sinica* 1987; 8(11): 579-586. [in Chinese]
- [8] Shinar J, Shima T. Robust missile guidance law against highly maneuvering targets. *Proceedings of the 7th Mediterranean Conference on Control and Automation*, 1999; 1548-1572.
- [9] Shinar J, Shima T. Nonorthodox guidance law development approach for intercepting maneuvering targets. *Journal of Guidance, Control, and Dynamics* 2002; 25(4): 658-666.
- [10] Shima T, Shinar T. Time-varying pursuit-evasion game models with bounded controls. *Journal of Guidance, Control, and Dynamics* 2002; 25(3): 425-432.
- [11] Shima T, Shinar T, Weiss H. New interceptor guidance law integrating time-varying and estimation-delay models. *Journal of Guidance, Control, and Dynamics* 2002; 25(4): 295-303.
- [12] Li Y Q, Qi N M, Sun X L, et al. Game space decomposition study of differential game guidance law for endoatmospheric interceptor missiles. *Acta Aeronautica et Astronautica Sinica* 2010; 31(8): 1600-1607. [in Chinese]
- [13] Li Y Q, Qi N M, Zhang W H, et al. Bounded differential game guidance law for interceptor missiles with aero-fins and reaction-jets. *Transactions of the Japan Society for Aeronautical and Space Sciences* 2011; 53(182): 275-282.
- [14] Liu Y F, Qi N M, Xia Q, et al. Differential game guidance law for endoatmospheric interceptor missiles based on nonlinear model. *Acta Aeronautica et Astronautica Sinica* 2011; 32(7): 1171-1179. [in Chinese]
- [15] Perelman A, Shima T, Rusnak I. Cooperative differential games strategies for active aircraft protection from a homing missiles. *Journal of Guidance, Control, and Dynamics* 2011; 34(3): 761-773.
- [16] Shima T. Optimal cooperative pursuit and evasion strategies against a homing missile. *Journal of Guidance, Control, and Dynamics* 2011; 34(2): 414-425.
- [17] Foley M, Schmitendorf W. A class of differential games with two pursuers versus one evader. *IEEE Transactions on Automatic Control* 1973; 19(3): 239-243.
- [18] Lin W, Qu Z H, Simaan A M. A design of distributed nonzero-sum Nash strategies. *49th IEEE Conference on Decision and Control*, 2010: 6305-6310.
- [19] Shima T, Golan M O. Heas pursuit guidance. *Journal of Guidance, Control, and Dynamics* 2007; 30(5): 1437-1444.
- [20] Shima T. Deviated velocity pursuit. *AIAA-2007-6782*, 2007.
- [21] Qi N M, Liu Y F, Sun X L. Differential game guidance law for interceptor missiles with a time-varying lateral acceleration limit. *Transactions of the Japan Society for Aeronautical and Space Sciences* 2011; 54(185): 189-197.
- [22] Zanchan P. Tactical and strategic missile guidance. 2nd ed. *Progress in Astronautics and Aeronautics*, 2002, 157: 181-202.
- [23] Dionne D, Michalska H, Shinar J, et al. Decision-directed adaptive estimation and guidance for an interception endgame. *Journal of Guidance, Control, and Dynamics* 2006; 29(4): 970-980.

Biography:

LIU Yanfang is a Ph.D. student at School of Astronautics, Harbin Institute of Technology. He received his B.S. degree from the Harbin Engineering University in 2008. His area of research includes missile guidance and control.
E-mail: liu-yanfang@hotmail.com